Avogado Nuts Extract (ANE) : An efficient Inhibitor of C38 Steel Corrosion in Hydrochloric Acid

**M. Belkhaouda[1], L. Bammou[1], R. Salghi[1*], O. Benali[2], A. Zarrouk[3],
Eno E. Ebenso[4], B. Hammouti[3,5]**

[1] *Equipe de Génie de l'Environnement et Biotechnologie, ENSA, Université Ibn Zohr, BP1136 Agadir, Morocco.*
[2] *Départment de Biologie, Faculté des sciences et de la technologie, Université Dr. Tahar Moulay – Saïda - Algérie*
[3] *LCAE-URAC18, Faculté des Sciences, Université Mohammed 1er, Oujda, Morocco.*
[3] *Material Science Innovation & Modelling (MaSIM) Focus Area, Faculty of Agriculture, Science and*
[4] *Technology, North-West University (Mafikeng Campus), Private Bag X2046, Mmabatho 2735, South Africa*
[5] *Petrochemical Research Chair, Chemistry Department, College of Science, King Saud University, P.O. Box 2455, Riyadh 11451, Saudi Arabia.*

Abstract

The inhibitive action of Avogado Nuts Extract (**ANE**) on C38 steel in 1M HCl solution was studied using potentiodynamic polarization and electrochemical impedance spectroscopy (EIS). The extracts were found to inhibit the corrosion of C38 steel in 1M HCl. The inhibition efficiency increased with the extracts concentration. Polarization curves reveal that **ANE** is a mixed type inhibitor with predominant cathodic effectiveness. Changes in impedance parameters (charge transfer resistance, R_t, and double-layer capacitance, C_{dl}) were indicative of adsorption of **ANE** on the metal surface, leading to the formation of a protective film. The effect of the temperature on the corrosion behaviour with addition of the optimal concentration of **ANE** was studied in the temperature range 298 – 328 K. The inhibition efficiency of the plant extract remain slightly constant with increasing temperature. Adsorption of **ANE** on the C38 steel surface is found to obey the Langmuir adsorption isotherm. Some thermodynamic functions of dissolution process were also determined.

Keywords: Avogado Nuts Extract, corrosion, inhibition, C38 steel, adsorption.

1. Introduction

Acid solutions generally used for the removal of rust and scale in industrial processes and the deterioration of the metal due to these processes are very significant. Inhibitors are used in these processes to control the metal dissolution. Hydrochloric acid is widely used in the pickling of steel and different steel based alloys [1–2]. One way of protecting steel from corrosion is to use corrosion inhibitors. Organic compounds containing heteroatoms are commonly used to reduce the corrosion attack on steel in acidic media [3-16]. Many industrial processes have put to use inorganic inhibitors for corrosion protection but as a result of cost and toxicity, attention is currently shifted towards the use of more eco-friendly inhibitors [17-18]. Organic substances *(plant based)* containing functional groups with oxygen, nitrogen and /or sulphur atoms in a conjugate system have been reported to exhibit good inhibiting properties [19-21]. This has made plant extracts an important choice for environmentally friendly, readily available and renewable source for wide range of inhibitors referred to as green inhibitors [22]. Some of the advantages of green inhibitors are low cost of processing, biodegradability, and absence of heavy metals or other toxic compounds which pose great hazard to the environment [23]. These advantages have incited us to draw a large part of program of our laboratory to examine natural substances as corrosion inhibitors [24-46].
The aim of the present work was established to study the corrosion inhibition of C38 steel in 1M HCl solution by Avogado Nuts Extract (**ANE**) as corrosion inhibitor using potentiodynamic polarization and electrochemical impedance spectroscopy (EIS).

2. Materials and methods

2. 1. Solutions preparation

Stock solution of the avogado nuts Extract (**ANE**) was prepared by stirring cold weighed amounts of the avogado nuts for 24 h in 1 M HCl solution. The resulting solution was filtered. This extract of this avogado nuts was used to study the corrosion inhibition properties and to prepare the required concentrations. The solution tests are freshly prepared before each experiment.

2. 3. Electrochemical tests

The electrochemical study was carried out using a potentiostat PGZ100 piloted by Voltamaster software. This potentiostat is connected to a cell with three electrode thermostats with double wall (Tacussel Standard CEC/TH). A saturated calomel electrode (SCE) and platinum electrode were used as reference and auxiliary electrodes, respectively. The material used for constructing the working electrode was the same used for gravimetric measurements. The surface area exposed to the electrolyte is 0.04 cm^2. Potentiodynamic polarization curves were plotted at a polarization scan rate of 0.5 mV/s. Before all experiments, the potential was stabilized at free potential during 30 min. The polarisation curves are obtained from –800 mV to –100 mV at 298 K. The solution test is there after de-aerated by bubbling nitrogen. Gas bubbling is maintained prior and through the experiments. In order to investigate the effects of temperature and immersion time on the inhibitor performance, some test were carried out in a temperature range 298–328 K.

The electrochemical impedance spectroscopy (EIS) measurements are carried out with the electrochemical system (Tacussel), which included a digital potentiostat model Voltalab PGZ100 computer at E_{corr} after immersion in solution without bubbling. After the determination of steady-state current at a corrosion potential, sine wave voltage (10 mV) peak to peak, at frequencies between 100 kHz and 10 mHz are superimposed on the rest potential. Computer programs automatically controlled the measurements performed at rest potentials after 0.5 hour of exposure at 298 K. The impedance diagrams are given in the Nyquist representation. Experiments are repeated three times to ensure the reproducibility.

Inhibition efficiencies (%) were calculated as follows:

- *For impedance measurements:*

$$EI_{Rt} (\%) = \frac{R_t - R_t^0}{R_t} \times 100 \tag{1}$$

where R_t and R_t^0 are the charge transfer resistance values without and with inhibitor, respectively.

- *For potentiodynamic polarisation measurements*:

$$EI_{Icorr} (\%) = \frac{I_{corr}^0 - I_{corr}}{I_{corr}^0} \times 100 \tag{2}$$

where I_{corr} and I'_{corr} are the corrosion current densities in the absence and the presence of the inhibitor.

3. Results and discussion

3.1. Effect of concentration

3. 1. 1. Electrochemical impedance spectroscopy measurements

The corrosion behaviour of C38 steel, in acidic solution in the presence of **ANE**, was investigated by the EIS methods at 298 K. Nyquist plots obtained for frequencies ranging from 100 kHz to 10 mHz at open circuit potential for C38 steel in 1 M HCl in the presence of various concentrations of **ANE** are shown in Figure 1. The impedance diagrams obtained are not perfect semicircles and the difference was attributed to frequency dispersion [47]. The fact that impedance diagrams have a semicircular appearance shows that the corrosion of C38 steel is controlled by a charge transfer process. The equivalent circuit model employed for this system is presented in Figure 2. The resistance R_s is the resistance of the solution; R_t reflects the charge transfer resistance and C_{dl} is the double - layer capacitance. The circuit consists of a constant phase element (CPE) Q, in parallel with a resistor R_t The use of CPE-type impedance has been extensively described in [14–15]:

$$Z_{CPE} = [Q(jw)^n]^{-1} \tag{3}$$

The above equation provides information about the degree of non-ideality in capacitance behavior. Its value makes it possible to differentiate between the behavior of an ideal capacitor (n = 1) and of a CPE (n < 1). Considering that a CPE may be considered as a parallel combination of a pure capacitor and a resistor that is inversely proportional to the angular frequency, the value of capacitance, C_{dl}, can thus be calculated for a parallel circuit composed of a CPE (Q) and a resistor (R_t), according to the following formula [16, 50]:

$$Q = (C_{dl}R_t)^n/R_t \qquad (4)$$

The impedance spectra were analyzed by using the circuit in figure 2, and the double layer capacitance (C_{dl}) was calculated in terms of Eq. 4. Values of elements of the circuit corresponding to different corrosion systems, including values of C_{dl}, are listed in Table 1.

This inductive arc is generally attributed to anodic adsorbed intermediates controlling the anodic process [48-49].
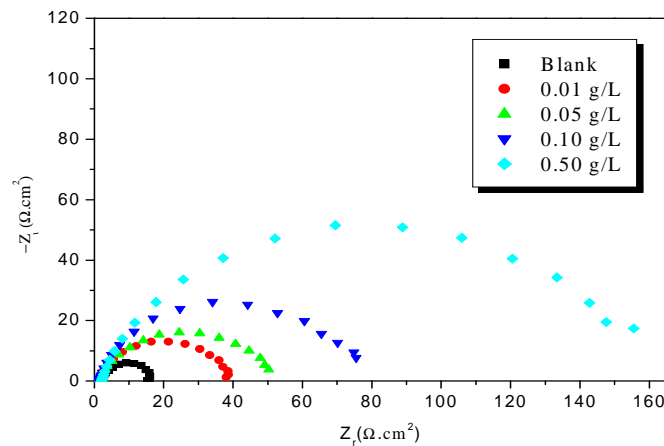

Figure 1. Nyquist plots of C38 steel in 1M HCl without and with different concentrations of **ANE** at 298 K.
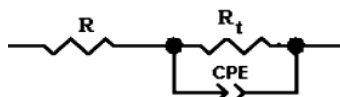

Figure 2. The equivalent circuit of the impedance spectra obtained for **ANE**.

Table 1 Impedance parameters for C38 steel in 1M HCl without and with different concentrations of **ANE** at 298 K.

Conc. (g/L)	R_t ($\Omega.cm^2$)	n	Q (Sn /$\Omega.cm^2$)	C_{dl} ($\mu F.cm^{-2}$)	IE_{Rt} (%)
Blank	15	0.86	1.65×10^{-4}	62	-----
0.01	41	0.84	1.35×10^{-4}	50	**63.41**
0.05	53	0.80	1.30×10^{-4}	37	**71.70**
0.1	80	0.84	7.49×10^{-5}	28	**81.25**
0.5	160	0.81	7.31×10^{-5}	26	**90.63**

The examination of the results of table 1 enables us to deduce the following points:

- The R_t values increased with the increasing concentration of the inhibitor indicating that more inhibitor molecule adsorb on the metal surface at higher concentration and form a protective film on the metal–solution interface [51-52].
- The value of C_{dl} decreased with increasing inhibitor concentration. Decrease of C_{dl} may be caused by a reduction in local dielectric constant and/or by an increase in the thickness of the electrical double layer. These results indicate that the inhibitor act by adsorption on the metal/solution interface [53-54]. These observations suggest that **ANE** inhibitor function by adsorption at the metal surface and thereby causing a decrease in the C_{dl} values and an increase in the R_t values.
- The value of n decreases as well (0.84–0.80), when compared to that obtained in pure HCl. This can be attributed to a certain increase of the initial surface inhomogeneity resulting from the inhibitor's adsorption on the most active centers.
- The inhibiting effectiveness increases with the concentration of the inhibitor to reach a maximum value from 90.63% to 0.5 g/L.

3. 1. 2. Polarization measurements

Figure 3 shows the polarisation curves of C38 steel in 1 M HCl and in the presence of different concentrations (0.02 – 0.5 g/L) of **ANE**. With the increase of **ANE** concentrations, both anodic and cathodic currents were inhibited. This result shows that the addition of **ANE** reduces anodic dissolution and also retards the hydrogen evolution reaction. Table 2 gives the values of kinetic corrosion parameters as the corrosion potential E_{corr}, corrosion current density I_{corr}, Tafel slope b_c, and inhibition efficiency for the corrosion of C38 steel in 1M HCl with different concentrations of **ANE**.
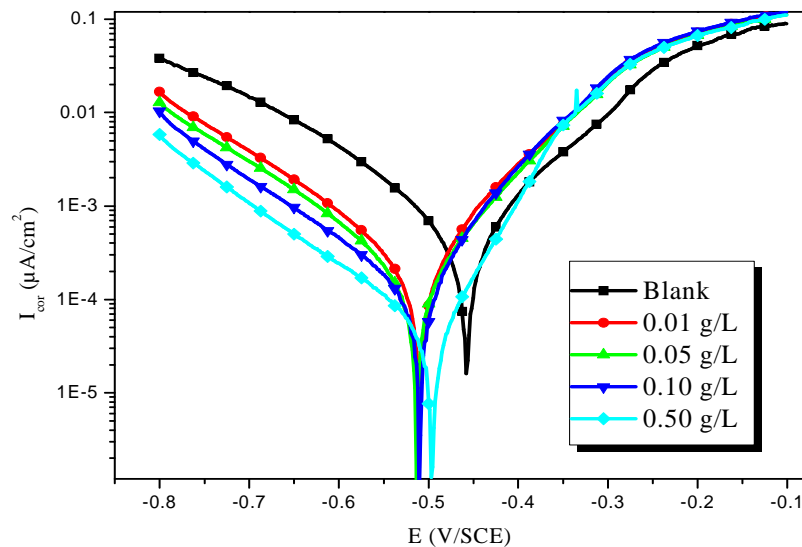

Figure 3. Polarization curves for C38 steel in 1 M HCl at various concentrations of **ANE** at 298K.

Table 2. Electrochemical parameters of C38 steel in 1M HCl at different concentration of **ANE** at 298K.

Conc. (g/L)	$I_{cor}(\mu A/cm^2)$	E_{corr} (mV/SCE)	b_c (mV/dec)	IE_{Icorr} (%)
Blank	594	-457	-199	-
0.01	263	-513	-159	**55.72**
0.05	205	-513	-161	**65.49**
0.10	133	-510	-161	**77.61**
0.50	53	-497	-159	**91.08**

The corrosion current densities were estimated by Tafel extrapolation of the cathodic curves to the open circuit corrosion potential. From table 2, it can be concluded that:

- The I_{corr} values decrease with increasing inhibitor concentration.
- The E_{corr} values were shifted toward the negative in the presence of the inhibitor. The presence of **ANE** in the acidic solution results in a slight shift of corrosion potential towards more negative in comparison to that in its absence, and the values of corrosion potential nearly remain constant with the addition of different concentration of **ANE**. These results indicate that **ANE** acts as a mixed-type inhibitor with predominant cathodic effectiveness. According to Ferreira [55], if the displacement in (E_{corr}) values (i) >85 mV in inhibited system with respect to uninhibited, the inhibitor could be recognized as cathodic or anodic type and (ii) if displacement in E_{corr} is <85 mV, it could be recognized as mixed-type. For studied inhibitor, the maximum displacement range was 56 mV towards cathodic region, which indicates that the studied **ANE** is mixed-type inhibitor [56-57].
- The cathodic Tafel slopes were found to vary over a range of 159-199 mV dec[-1]. Therefore, the cathodic slope value was found to change with increasing concentration of **ANE** in 1 M HCl . This result indicates the influence of the inhibitor on the kinetics of the hydrogen evolution reaction [13, 58].
- The values of inhibition efficiency (IE_{Icorr} %) increase with inhibitor concentration reaching a maximum value (91.08 %) at 0.5 g/L.

These polarisation curves measurements were in good agreement with the electrochemical impedance tests.

3. 2. Effect of temperature

The change of the corrosion process rate with the temperature increase was studied in 1M HCl in the absence and in the presence of inhibitor by potentiodynamic polarization (Figs. 4 and 5). Corresponding data are given in table 3. It's has been observed that the corrosion current density (I_{corr}) increased and the polarization resistance decreases with the increase in **ANE** increasing temperature. It is seen also that the **ANE** investigated have been inhibiting properties at all temperatures studied and the values of inhibition efficiency remain slightly constant with temperature increase.
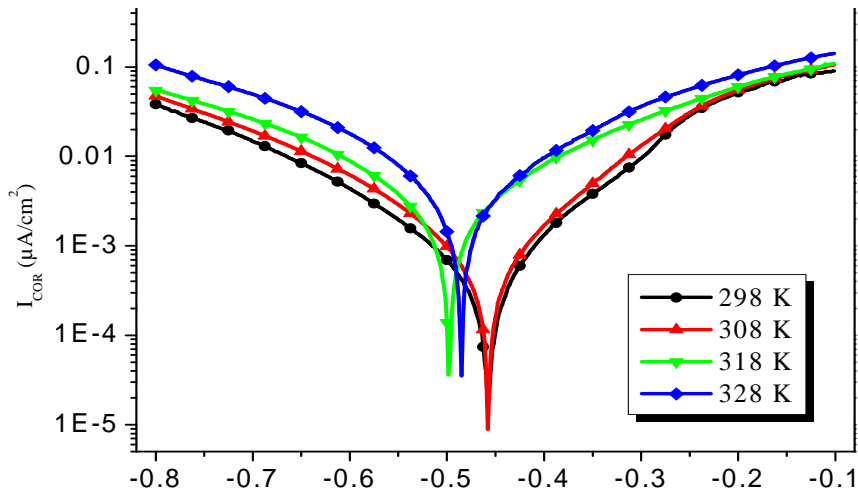

Figure 4. Polarisation curves for C38 in 1M HCl at different temperature
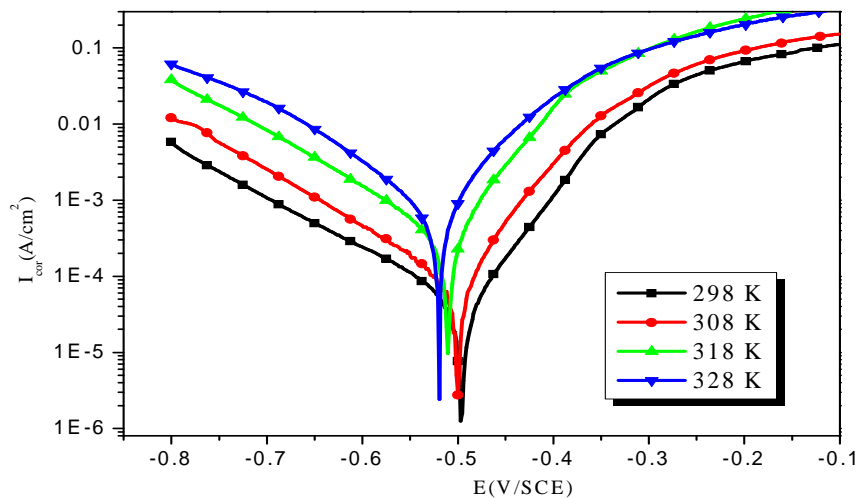

Figure 5. Polarisation curves for C38 in 1M HCl + 0.5g/L **ANE** at different temperatures

We were interested in exploring the activation energy of the corrosion process and the thermodynamics of adsorption of **ANE**. This was accomplished by investigating the temperature dependence of the corrosion current, obtained using Tafel extrapolation method. The corrosion reaction can be regarded as an Arrhenius-type process, the rate is given by:

$$\log I = -\frac{E_a}{2.303\,RT} + \log A \tag{5}$$

where E_a is the apparent activation corrosion energy, T is the absolute temperature, k is the Arrhenius pre-exponential constant and R is the universal gas constant.

This equation can be used to calculatethe E_a values of the corrosion reaction without and with **ANE**. Plotting the natural logarithm of the corrosion current density versus 1/T, the activation energy can be calculated from the slope.

Table 3. Electrochemical parameters for corrosion of C38 steel in 1M HCl at different temperatures in the absence and presence of 0.5 g/L **ANE**

Conc. (g/L)	T (K)	E_{cor} (mV/CSE)	I_{cor} (µA/cm^2)	bc (mV/dec)	E_p (%)
Blank	298	-457	594	-204	--
	308	-458	900	-199	--
	318	-500	3360	-214	--
	328	-487	6820	-234	--
0.5 g/L	298	-497	53	-159	91.08
	308	-500	87	-138	90.33
	318	-511	341	-139	89.85
	328	-520	717	-137	89.49

The temperature dependence of C38 steel dissolution in 1 M HCl and in the presence inhibitor is presented in Arrhenius co-ordinates in Fig. 6. The calculated values of the apparent activation corrosion energy in the absence and presence of **ANE** are listed in the Table 4.
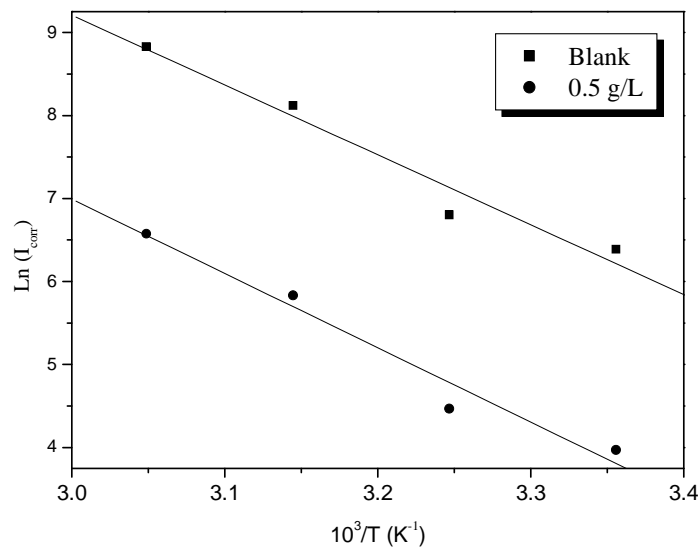

Figure 6. Arrhenius plots of C38 steel in 1 M HCl with and without 0.5 g/L of **ANE**

All the linear regression coefficients were close to one. The value of E_a found for **ANE** is higher than that obtained for 1 M HCl solution. The increase in the apparent activation energy may be interpreted as physical adsorption that occurs in the first stage [59-60]. Szauer and Brand [61] explained that the increase in activation energy can be attributed to an appreciable decrease in the adsorption of the inhibitor on the C38 steel surface with increase in temperature.

As adsorption decreases more desorption of inhibitor molecules occurs because these two opposite processes are in equilibrium. Due to more desorption of inhibitor molecules at higher temperatures, an important surface of C38 steel comes in contact with aggressive environment, resulting increased corrosion rates with increase in temperature [62].

An alternative formulation of Arrhenius equation is [63]:

$$I_{corr} = \frac{RT}{Nh} \exp(\frac{\Delta S_a^o}{R}) \exp(\frac{\Delta H_a^o}{RT}) \qquad (6)$$

where h is Planck's constant, N is Avagadro's number, ΔS_a is the entropy of activation and ΔH_a is the enthalpy of activation.

Fig. 7 shows a plot of ln (I_{corr}/T) vs. 1/T. Straight lines are obtained with a slope of ΔH_a/R and an intercept of ln R/Nh + ΔS_a/R from which the values of ΔS_a and ΔH_a are calculated and are given in Table 4.

Inspection of these data revealed that the thermodynamic parameters (ΔSa and ΔHa) for dissolution reaction of C38 steel in 1 M HCl in the presence of inhibitor are higher than that obtained in the absence of inhibitor. The positive sign of ΔHa reflects the endothermic nature of the C38 steel dissolution process suggesting that the dissolution of C38 steel is slow [64] in the presence of inhibitor. On comparing the values of the entropy of activation ΔSa given in table 4, it is clear that entropy of activation decreased positively in the presence of **ANE** than in the absence of inhibitor. The decrease of ΔSa reveals that an decrease in disordering takes place on going from reactant to the activated complex [65-66]. One can notice that Ea and ΔHa values vary in the same way (Table 4).
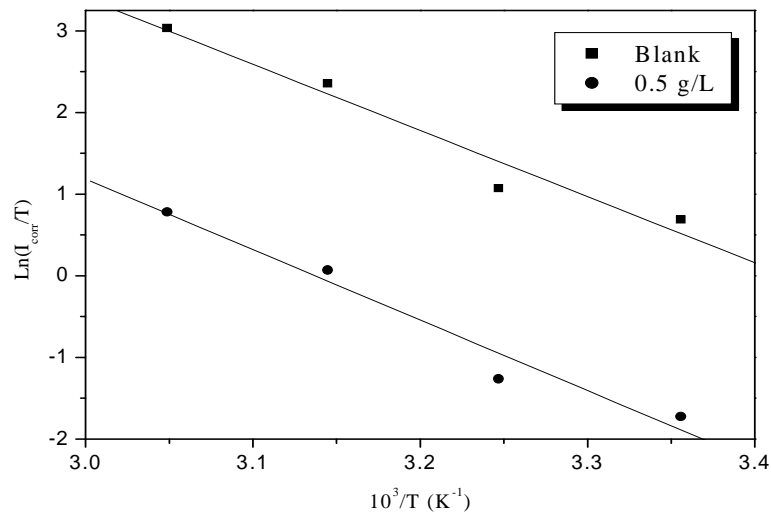

Figure 7. Variation of Ln (I_{corr}/T) versus $10^3/T$ for blank and 1M HCl + 0.5 g/L **ANE**

Table 4. Activation parameters Values for C38 steel in 1M HCl in the absence and presence of 0.5 g/L of **ANE**

	E_a (kJ mol^{-1})	ΔH_a (kJ mol^{-1})	ΔS_a (J mol^{-1} K^{-1})
Blank	70.01	67.41	32.97
0.5 g/L	74.42	71.82	27.78

3. 3. Adsorption isotherm and mechanism of inhibition

Adsorption isotherms are very important to understand the mechanism of inhibition corrosion reactions. The most frequently used isotherms are Langmuir [67], Frumkin [68] and Temkin [69]. The Langmuir isotherm (C/θ vs C) assumes that there is no interaction between adsorbed molecules on the surface. The Frumkin adsorption isotherm (θ vs C) assumes that there is some interaction between the adsorbates, and the Temkin adsorption isotherm (θ vs lgC) represents the effect of multiple layer coverage [70]. Figure 8 shows the dependence of C/ θ as function of the of **ANE** concentration. The curve obtained clearly shows that the data fit well with Langmuir adsorption isotherm was found to be the best description of the adsorption behavior of the studied inhibitor, which obeys:
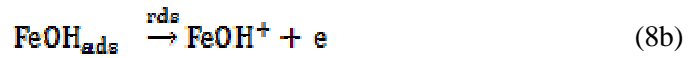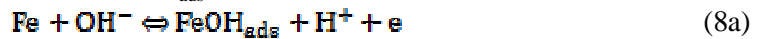
$$\frac{C}{\theta} = \frac{1}{K} + C \qquad (7)$$

Where C is the concentration of inhibitor, K is the equilibrium constant of the adsorption process, and θ is the surface coverage.

This suggests that extract in present study obeyed the Langmuir isotherm and there is negligible interaction between the adsorbed molecules.

The observed corrosion inhibition of C38 steel in HCl solution with increase in **ANE** concentration can be explained by the adsorption of the components of the **ANE** on the metal surface. In order to predict the type of adsorption, the corrosion mechanism of the iron must be known. According to the mechanism for the anodic
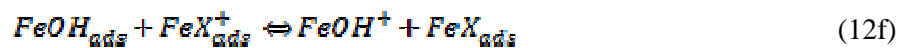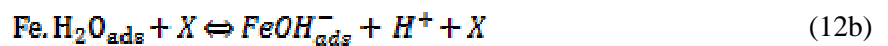
dissolution of Fe in acidic solutions proposed by several authors [71-72], Fe electro-dissolution in acidic solutions depends primarily on the adsorbed intermediate $FeOH_{ads}$ as follows:

$$Fe + OH^- \rightleftharpoons FeOH_{ads} + H^+ + e \tag{8a}$$

$$FeOH_{ads} \overset{rds}{\rightarrow} FeOH^+ + e \tag{8b}$$

$$FeOH^+ + H^+ \rightleftharpoons Fe^{2+} + H_2O \tag{8c}$$

The cathodic hydrogen evolution follows the steps :

$$Fe + H^+ \rightleftharpoons (FeH^+)_{ads} \tag{9}$$

$$(FeH^+)_{ads} + e \rightleftharpoons (FeH)_{ads} \tag{10}$$

$$(FeH)_{ads} + H^+ + e \rightarrow Fe + H_2 \tag{11}$$

The corrosion rate of C38 steel in HCl solutions is controlled by both hydrogen evolution reaction and dissolution reaction of iron. Another mechanism, involving two adsorbed intermediates has been used to account for the retardation of Fe anodic dissolution in the presence of an inhibitor [73] :

$$Fe + H_2O \rightleftharpoons Fe.H_2O_{ads} \tag{12a}$$

$$Fe.H_2O_{ads} + X \rightleftharpoons FeOH^-_{ads} + H^+ + X \tag{12b}$$

$$Fe.H_2O_{ads} + X \rightleftharpoons FeX_{ads} + H_2O \tag{12c}$$

$$FeOH^-_{ads} \overset{rds}{\rightarrow} + FeOH_{ads} + e \tag{12d}$$

$$FeX_{ads} \rightleftharpoons FeX^+_{ads} + e \tag{12e}$$

$$FeOH_{ads} + FeX^+_{ads} \rightleftharpoons FeOH^+ + FeX_{ads} \tag{12f}$$

$$FeOH^+ + H^+ \rightleftharpoons Fe^{2+} + H_2O \tag{12g}$$
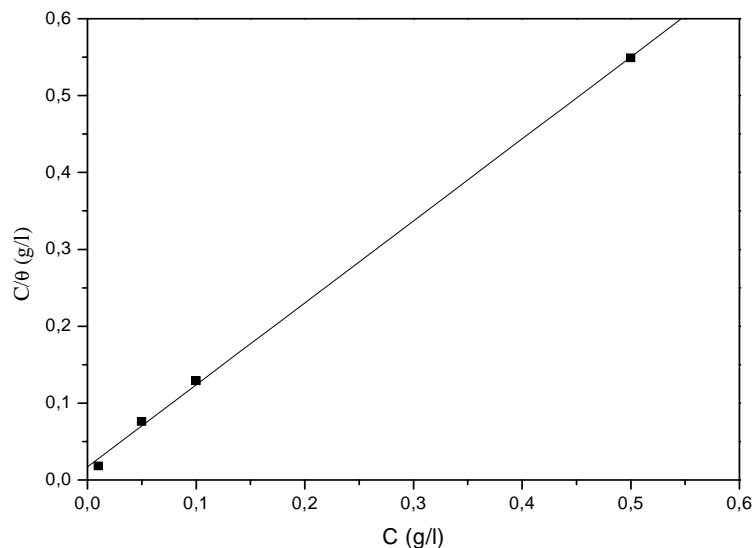
where X represents the inhibitor species.

Figure 8. Langmuir isotherme adsorption of **ANE** on the C38 steel in 1M HCl obtained by polarization curves

According to the detailed mechanism above, displacement of some adsorbed water molecules on the metal surface by inhibitor species to yield the adsorbed intermediate FeYads (Eq. (12c)) reduces the amount of the species $FeOH^-_{ads}$ available for the rate determining step. Such adsorbed intermediate could, depending on its relative solubility, either inhibit or catalyse further metal dissolution.

Conclusion

It can be concluded as follows:

- The Avogado Nuts Extract (**ANE**) was found to perform in 1M HCl.
- Polarization studies showed that the compound under investigation was mixed type inhibitor.
- The inhibition efficiency of **ANE** increased with the concentration and reached a maximum at 0.5 g / L.
- The EIS and polarization curves were in good agreement.
- Adsorption of **ANE** on the C38 steel surface from 1M HCl followed the Langmuir isotherm.
- The inhibition efficience of **ANE** remain slightly constant with increasing temperature and their addition led to increase of the activation corrosion energy.

References

1. Bentiss F., Gassama F., Barbry D., Gengembre L., Vezin H., Lagreneée M., Traisnel M. *Appl. Surf. Sci.* 252 (2006) 2684.
2. Khaled K. F., Hackerma N. *Electrochim. Acta.* 48 (2003) 2715.
3. Mihit M., El Issami S., Bouklah M., Bazzi L., Hammouti B., Ait Addi E., Salghi R., Kertit S. *Appl. Suf. Sci.* 252 (2006) 2389.
4. Hammouti B., Salghi R., Kertit S. *J. Electrochem. Soc. India.* 47 (1998) 31.
5. Zarrok H., Oudda H., Zarrouk A., Salghi R., Hammouti B., Bouachrine M. *Der Pharma Chem.* 3 (2011) 576
6. El Issami S., Bazzi L., Mihit M., Hilali M., Salghi R., Ait Addi El. *J. Phys. IV.* 123 (2005) 307.
7. El Issami S., Bazzi L., Mihit M., Hammouti B., Kertit S., Ait Addi E., Salghi R. *Pig. Res. Tech.* 36 (2007) 161
8. Mihit M., Laarej K., Abou El Makarim H., Bazzi L., Salghi R., Hammouti B. *Arab. J. Chem.* 3 (2010) 55.
9. Mihit M., Salghi R., El Issami S., Bazzi L., Hammouti B., Ait Addi El., Kertit S. *Pig. Res. Tech.* 35 (2006) 151
10. Barouni K., Bazzi L., Salghi R., Mihit M., Hammouti B., Albourine A., El Issami S. *Mater. Lett.* 62 (2008) 3325.
11. El Issami S., Bazzi L., Hilali M., Salghi R., Kertit S. *Ann. Chim. Sci. Mat.* 27 (2002) 63.
12. Salghi R., Bazzi L., Hammouti B., Kertit S. *Bull. Electrochem.* 16 (2000) 272.
13. Benali O., Larabi L., Tabti B., Harek Y., *Anti-corr. Meth. Mater.* 52 (2005) 280.
14. Benali O., Larabi L., Mekelleche S. M., Harek Y. *J. Mater. Sci.* 41 (2006) 7064.
15. Benali O., Larabi L., Harek Y. *J. Appl. Electrochem.* 39 (2009) 769.
16. Merah S., Larabi L., Benali O., Harek Y. *Pig. Res. Tech.* 37 (2008) 291.
17. Alaneme K. K., Olusegun S. J. *Leonardo J. Sci.* 20 (2012) 59-70.
18. Orubite K.O., Oforka N.C. *Mater. Lett.* 58 (2004)1768.
19. El-Etre A.Y., Abdallah M., El-Tantawy Z.E. *Corros. Sci.* 47 (2004) 385.
20. El-Etre P.B. *Appl. Surf. Sci.* 252 (2006) 8521.
23. Ebenso E.E., Eddy N.O., Odiongenyi A.O. *Afric J. Pure Appl. Chem.* 29(11) (2008) 107.
24. Lahhit N., Bouyanzer A., Desjobert J. M., Hammouti B., Salghi R., Costa J., Jama C., Bentiss F., Majidi L. *Port. Electrochim. Acta* 29 (2011) 127.
25. Ben Hmamou D., Salghi R., Bazzi Lh., Hammouti B., Al-Deyab S.S., Bammou L., Bazzi L., Bouyanzer A. *Int. J. Electrochem. Sci.* 7 (2012) 1303.
26. Afia L., Salghi R., Bazzi El., Bazzi L., Errami M., Jbara O., Al-Deyab S. S, Hammouti B. *Int. J. Electrochem. Sci.* 6 (2011) 5918.
27. Afia L., Salghi R., Bammou L., Bazzi Lh., B. Hammouti, L. Bazzi. *Acta Metall. Sin.* 25 (2012) 10.
28. Afia L., Salghi R., Bazzi El., Zarrouk A., Hammouti B., Bouri M., Zarrouk H., Bazzi L., Bammou L. *Res. Chem. Intermed.* (2012) ; DOI 10.1007/s11164-012-0496-y
29. Afia L., Salghi R., Bammou L., Bazzi El., Hammouti B., Bazzi L., Bouyanzer A. *J. Saud. Chem. Soc.* (2011), DOI:10.1016/j.jscs.2011.05.008
30. Afia L., Salghi R., Bazzi El., Bazzi L., Errami M., Jbara O., Al-Deyab S. S., Hammouti B. *Int. J. Electrochem. Sci.* 6 (2011) 5918.
31. Chetouani A., Hammouti B., Benkaddour M. *Res. Pig. Tech.* 33 (2004) 26.
32. El Ouariachi E., Paolini J., Bouklah M., Elidrissi A., Bouyanzer A., Hammouti B., Desjobert J-M., Costa J. *Acta Metall. Sin.* 23 (2010) 13.
33. Bendahou M., Benabdallah M., Hammouti B. *Pig. Res. Techn.* 35 (2006) 95.
34. Bouyanzer A., Hammouti B. *Bull. Electrochem.* 20 (2004) 63.

35. Bammou L., Chebli B., Salghi R., Bazzi L., Hammouti B., Mihit M., El Idrissi H. *Green Chem. Lett. Rev.* 3 (2010) 173.
36. Bouyanzer A., Hammouti B., Majidi L. *Mater. Lett.* 60 (2006) 2840.
37. Zerga B., Sfaira M., Rais Z., Ebn Touhami M., Taleb M., Hammouti B., Imelouane B., Elbachiri A. *Mater. Tech.* 97 (2009) 297.
38. Bouyanzer A., Hammouti B. *Pigm. Resin Techn.*, 33 (2004) 287.
39. Benabdellah M., Hammouti B., Benkaddour M., Bendahhou M., Aouniti A. *Appl. Surf. Sci.* 252 (2006) 6212.
40. Bammou L., Mihit M., Salghi R., Bazzi L., Bouyanzer A., Hammouti B. *Int. J. Electrochem. Sci.* 6 (2011) 1454.
41. Ouachikh O., Bouyanzer A., Bouklah M., Desjobert J-M., Costa J., Hammouti B., Majidi L. *Surf. Rev. Lett.* 6 (2009) 49.
42. Benali O., Benmehdi H., Hasnaoui O., Selles C., Salghi R. *J. Mater. Environ. Sci.* 4 (1) (2013) 127.
43. Benali O., C. Selles, R. Salghi. *Res. Chem. Intermed.* DOI 10.1007/s11164-012-0960-8.
44. Ben Hmamou D., Salghi R., Zarrouk A., Zarrok H., Benali O., Errami M., Hammouti B. *Res. Chem. Intermed.* DOI 10.1007/s11164-012-0840-2.
45. Afia L., Salghi R., Zarrouk A., Zarrok H., Benali O., Hammouti B., Al-Deyab S.S., Chakir A., Bazzi L. *Portug. Electrochim. Acta* 30(4) (2012) 267.
46. Ben Hmamou D., Salghi R., Zarrouk A., Benali O., Fadel F., Zarrok H., Hammouti B. *Internat. J. Indus. Chem.* 3(2012) 25.
47. Benali O., Larabi L., Traisnel M., Gengembre L., Harek Y. *Appl. Surf. Sci.* 253 (2007) 6130.
48. Caprani A., Epelboin I., Morel P. On Corros. Inhibitors, Ferrara, Italy (1975) 571.
49. Bessone J., Mayer C., Tuttner K., Lorenz W. J. *Electrochim. Acta.* 28 (1983)171.
50. Ma H., Chen S., Yin B., Zhao S., Liu X. *Corros. Sci.* 45 (2003) 867.
51. Bentiss F., Traisnel M., Lagrenee M. Corros. *Sci.* 42 (2000) 127.
52. Murlidharan S., Phani K. L. N., Pitchumani S., Ravichandran S. *J. Electrochem. Soc.* 142 (1995) 1478.
53. Abdel Rehim S. S., Hazzazi O. A., Amin M. A., Khaled F. K. *Corros. Sci.* 50 (2008) 2258.
54. Sorkhabi A. H., Seifzadeh D., Hosseini M. G. *Corros. Sci.* 50 (2008) 3363.
55. Ferreira E.S., Giancomelli C., Giacomelli F.C., Spinelli A. *Mater. Chem. Phys.* 83 (2004) 129.
56. Sorkhabi H.A., Shaabani B., Seifzadeh D. *Appl. Surf. Sci.* 239 (2005) 154.
57. Yadav D. K., Maiti B., Quraishi M.A. *Corros. Sci.* 52 (2010) 3586.
58. Lagrenée M., Mernari B., Bouanis M., Traisnel M., Bentiss F. *Corros. Sci.* 44 (2002) 573.
59. Lebrini M., Robert F., Lecante A., Roos C. *Corros. Sci.* 53 (2011) 687.
61. Martinez S., Stern I. *Appl. Surf. Sci.* 199 (2002) 83.
62. Szauer T., Brand A. *Electrochim. Acta* 26 (1981) 1219.
63. Bockris J.O'M., Reddy A.K.N., Modern Electrochemistry, vol. 2, Plenum Press, New York, (1977).
64. Guan N.M., Xueming L., Fei L. *Mater. Chem. Phys.* 86 (2004) 59.
65. Frignani A., Tassinari M., in: Proceedings of the Sixth European Symposium on Corrosion Inhibitors, Ann. Univ. Ferrara (1990) 895.
66. Rekkab S., Zarrok H., Salghi R., Zarrouk A., Bazzi Lh., Hammouti B., Kabouche Z., Touzani R., Zougagh M. *J. Mater. Environ. Sci.* 3 (4) (2012) 613.
67. Langmuir I. *J. Am. Chem. Soc.* 39 (1947) 1848.
68. Frumkin A.N.Z. *Phys. Chem.* 116 (1925) 466.
69. De Boer J.H., The Dynamical Character of Adsorption, second ed. Claredon Press, Oxford, UK, (1968).
70. R.I. Masel, Principles of Adsorption and Reaction on Solid Surfaces. Willey, New York, (1996).
71. Okafor P.C., Ikpi M.E., Uwaha I.E., Ebenso E.E., Ekpe U.J., Umoren S.A. *Corros. Sci.* 50 (2008) 2310.
72. Bockris J.O'M., Drazic D., Despic A.R. *Electrochim. Acta,* 4 (1961) 325.
73. Ashassi-Sorkhabi H., Nabavi-Amri S.A. *Acta Chim. Slov.* 47 (2000) 507.

(2013) ; http://www.jmaterenvironsci.com